

## Design and Preparation of Low Absorbing Antireflection Coatings Using Chemical Spray Pyrolysis

Salam A. Yousif<sup>1</sup>, Hayfa G.Rashid<sup>1</sup>, Khudheir A. Mishjil<sup>1</sup> and Nadir F. Habubi<sup>1\*</sup>

<sup>1</sup> Mustansiriyah university ,College of Education , Baghdad-Iraq.

Received 26 January 2018; Revised 15 June 2018; Accepted 26 June 2018

### ABSTRACT

*Transmission of laser optical elements has been increased when Indium tin oxide (ITO) thin film of relatively high index with different content of Sn was used to prepare ultra thin antireflection coating(ARC's) utilizing simple ,low cost non-vacuum chemical spray pyrolysis technique. Two plans were established to achieve the goal: theoretical transmission analysis of ITO film on glass was first carried on with the aid of TFCal software taking into account the effect of absorption, dispersion and ITO thickness variation on transmission profile. This step provides a clear vision and preliminary thickness range of ITO films before sample preparation with spray pyrolysis method. Results show that XRD spectra reveals that all the films were cubic polycrystalline. Both scanning electron microscope and atomic force microscope indicate that the surface roughness increase with Sn content. Thus , durable and adhesive antireflection ITO ultrathin film, of good transmittance profile was achieved at Nd-YAG laser line of 1.064  $\mu\text{m}$  wavelength when preparation conditions were optimum control .*

**Keywords:** Low Absorbing Antireflection Coating, Transfer Matrix Theory, ITO Material.

### 1. INTRODUCTION

Indium tin oxide (ITO) thin films have attracted intensive interest during the last four decades<sup>[1-11]</sup> their unique properties such as, high transparency in the visible range, high conductivity combined with low resistivity and high reflectivity, wide band gap of around 3.7 eV<sup>[12-15]</sup> made them usefull in industry. Owing to these properties indium tin oxide is used in many applications, especially light emitting diode<sup>[16,7]</sup>, gas sensors<sup>[18,19]</sup>, electrodes<sup>[20,21]</sup>, biosensor <sup>[22]</sup>, sound source devices<sup>[23]</sup>, resistive touch panel<sup>[24]</sup> and solar cells<sup>[25-28]</sup>.

Antireflection coatings (ARC's) are among the most investigated class of optical coatings. It is a type of optical coating or filters applied to the surface of lenses and other optical elements to reduce reflection. They are classified into a single layer of quarter-wave optical thickness ( $nd=\lambda_0/4$ ) having virtual zero reflectance at center ( design ) wavelength  $\lambda_0$  to multilayer having low reflectance over a broadband of wavelength<sup>[29-32]</sup>. Although the absorption of ITO was very low, mismatch exists between the refractive index of ITO ( $n\sim 2.0$ ) <sup>[33-35]</sup> and air ( $n=1.0$ ).This cause a significant reflection, particularly in the visible range, and consequently reduces visible transmittance. In this work, ITO film with low absorption characteristic was designed and prepared as antireflection coating using TFCal. <sup>[36]</sup> and spray pyrolysis solution to enhance near infrared transmittance of ITO/glass .

---

\*Corresponding Author : [nadirfadhil@uomustansiriyah.edu.iq](mailto:nadirfadhil@uomustansiriyah.edu.iq)

## 2. EXPERIMENTAL DETAILS

Indium tin oxide was deposited on an ultrasonically cleaned glass substrate using a proper, low cost, chemical spray pyrolysis technique. A precursor solution of deionized water with 0.05 M  $\text{InCl}_3$  supplied from (Thomas Baker Chemicals India) as a source of In, while 0.05 M of  $\text{SnCl}_4 \cdot 5\text{H}_2\text{O}$  supplied from (Chemical Point Germany) dissolve in deionized water was used as a province of Sn doping material of volumetric concentration 5% and 10% . The prepared solutions were appropriately mixed to obtain the starting solution and was sprayed immediately to preclude any potential chemical change with time. Many trials have been adopted in order to obtain homogeneous thin films, pinhole free and well adherent to the substrate. These optimization conditions were arrived at the following: the substrate temperature was electronically controlled by chromel alumel thermocouple and kept at 450 °C during the deposition process. The distance between substrate and nozzle was 28 cm , the carrier gas was nitrogen and was fixed at 3.5 Bar. The solution flow rate preserved at 5 ml/min, spraying time was 10 s followed by 2 min waiting to avert immoderate cooling.

The crystallinity of the films was examined by X-ray diffraction (XRD), while surface topography was estimated from atomic force microscopy (AFM) images. Surface morphology on the other hand was obtained by scanning electron microscope (SEM ). The optical spectra were recorded using (uv probe 1240 Schimadzu Japan) in the wavelength range (330-1100) nm.

### 2.1 Transfer Matrix Theory

We describe briefly the transfer matrix method [29-32] used to evaluate the reflectance and transmittance in addition to absorption and dispersion of layer film on a known substrate. For normal and near normal incidence the relationship between the magnitude of the electric  $E$  and magnetic  $H$  vectors in the medium of incidence [interface  $a$  in Figure 1 to that in the substrate of index  $n_s$  [interface  $b$  ] can be expressed as follows:

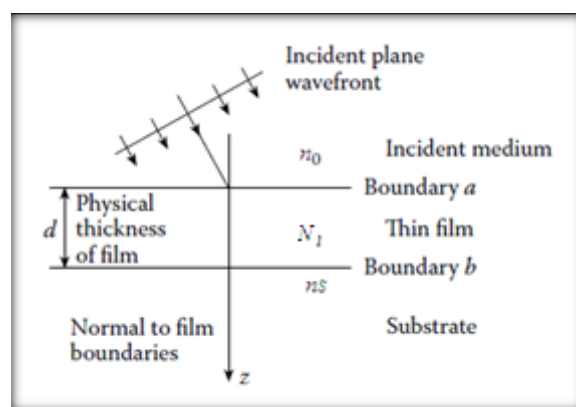


Figure 1. Plane waves incident on thin- film[27].

$$\begin{bmatrix} E_a \\ H_a \end{bmatrix} = \begin{bmatrix} \cos\delta & i\sin\delta/N_1 \\ iN_1\sin\delta & \cos\delta \end{bmatrix} \begin{bmatrix} E_b \\ H_b \end{bmatrix} \quad (1)$$

Where  $N_1 = n_1 - ik_1$  is the complex refractive index of the layer of thickness  $d_1$  .  $n_1$  and  $k_1$  are the refractive index and extinction coefficient .  $\delta = 2\pi N_1 d/\lambda$  is the phase thickness of the layer.

Adopting the "Input Optical Admittance" concept  $Y = \frac{H_a}{E_a}$ , the reflectance  $R$  and transmittance  $T$  of layer are:

$$R = \left( \frac{n_0 - Y}{n_0 + Y} \right) \left( \frac{n_0 - Y}{n_0 + Y} \right)^* \quad (2)$$

$$T = \frac{4n_0 Re(N)}{(n_0 + Y)(n_0 - Y)^*} \quad (3)$$

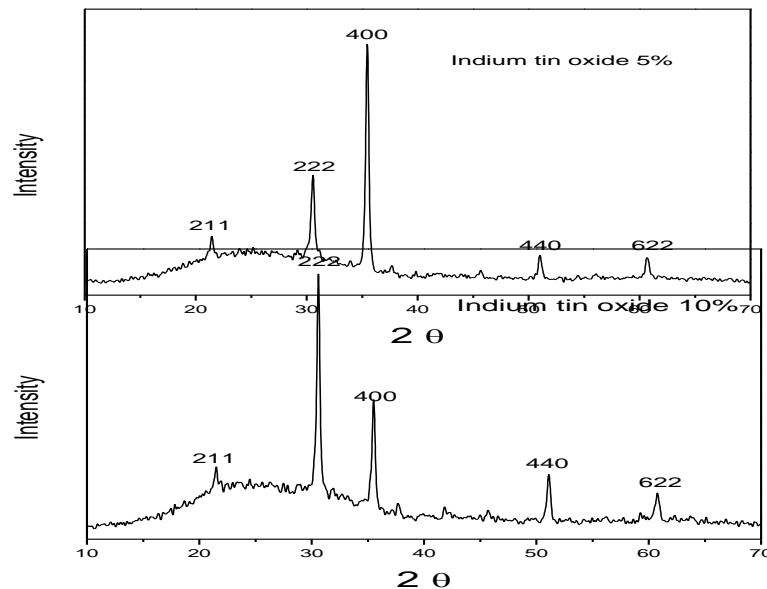
Where  $Re(N)$  represent the real part of  $N$ . For absorbing- free material ,the necessary condition of AR coating is :

$$n_1 = \sqrt{n_0 n_s} \quad \text{and} \quad n_1 d = \lambda_0 / 4 \quad (4)$$

### 3. RESULTS AND DISCUSSION

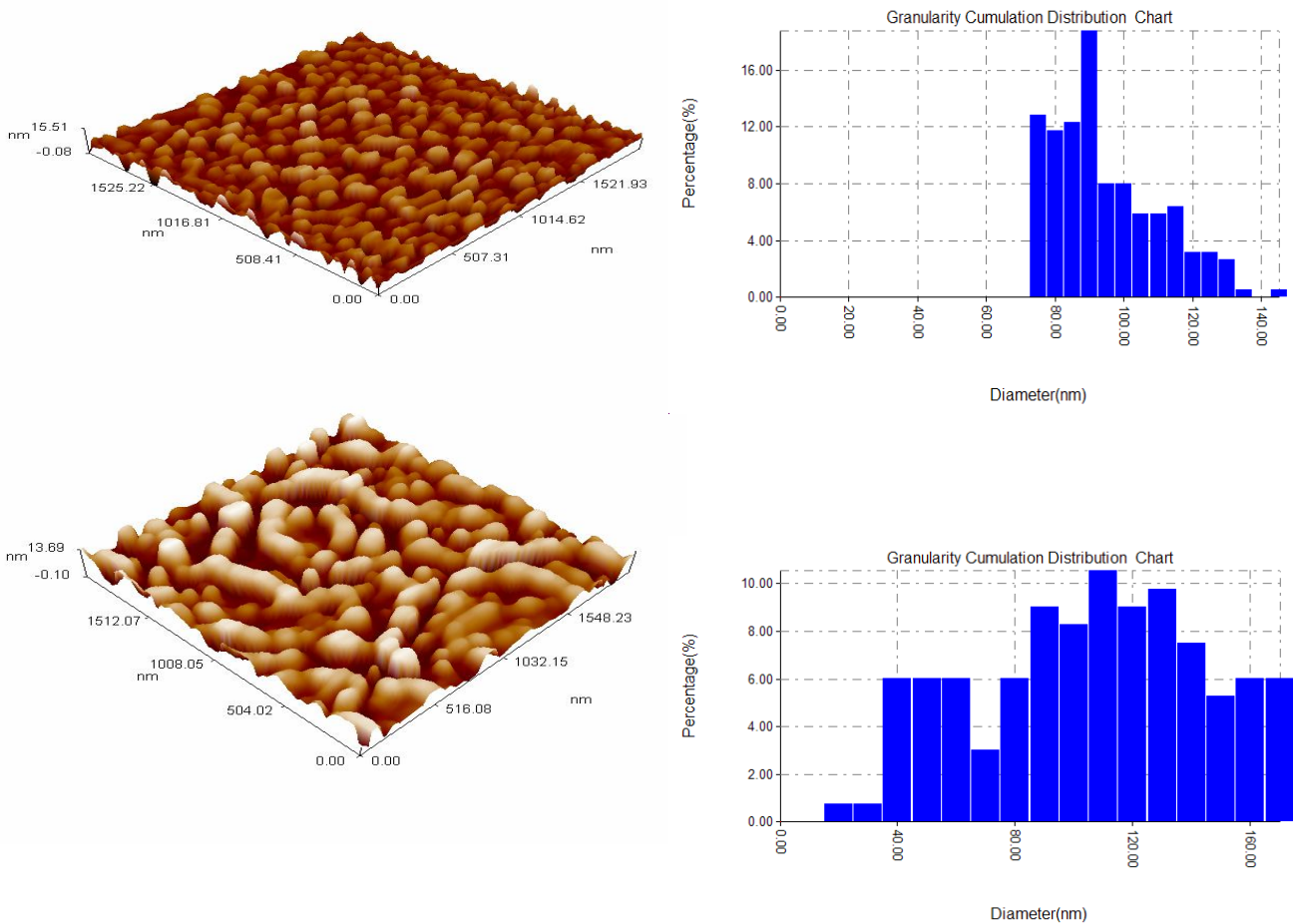
#### 3.1 Structural Properties

Figure 2 depicts the XRD patterns of the as deposited indium tin oxide with 5% and 10% Sn concentrations. These films show a major (222) and (400) planes ,with three minor peaks correspond to (211),(440) and (622) planes, indicating that the structure is cubic polycrystalline, which agrees with JCPDS card no. 06.0416. No trace for Sn or any of its oxide was observed in these patterns. It can be concluded that the tin atoms were likely being substitutionally doped into indium matrix. The prevalent orientation peak was changed from (400) to (222) as the Sn concentration increase. This might be due to the increase in the amount of incorporating oxygen [35]. The full width at half maximum decrease as the Sn concentration increase suggested that the grain size also increased.



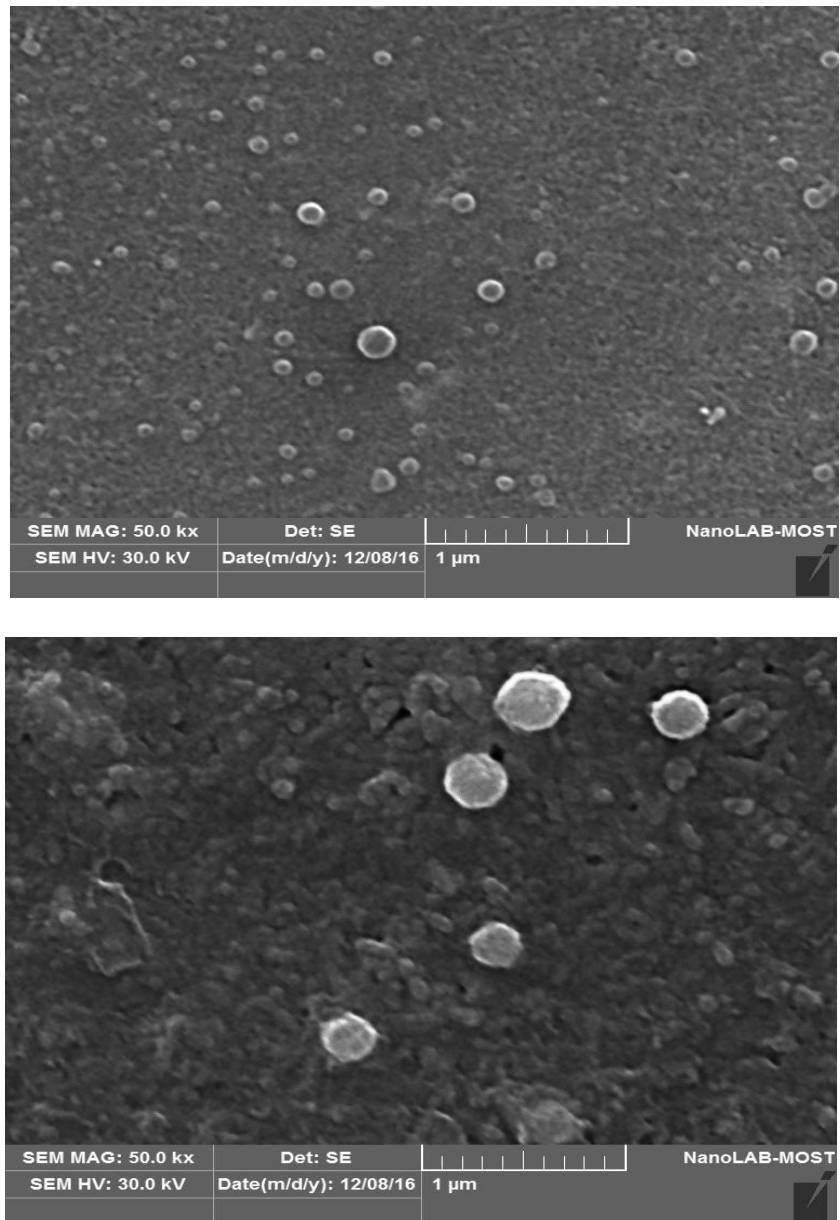
**Figure 2.** XRD patterns for indium tin oxide a) 5% Sn concentration b)10% Sn concentration.

Figure 3 shows AFM images of ITO with different Sn 5% and 10% content. It was noticed that the value of RMS roughness and the average grain size for Sn 5% which were equal to 2.14 nm and 92.39 nm respectively, increased to 3.11 nm and 101.74 nm as the Sn content increase to 10%.



**Figure 3.** AFM images of indium tin oxide a) 5% Sn concentration b) 10% Sn concentration.

SEM images show a fine and uniform distribution of grains as shown in Figure 4. There was a worthy change in these images because of tin concentration. It was observed that porosity decrease with the increase of grain size and Sn content.



**Figure 4.** SEM images of indium tin oxide a) 5% Sn concentration b)10% Sn concentration.

### 3.2 Theoretical Computation

TFCal. [36] was adopted to compute transmittance versus wavelength of ITO /Glass taken into account the effect of dispersion phenomena for  $n$  and  $k$  data taken from Refs. [33-35]. Further, the effect of thickness variation also studied at a different design wavelength:  $\lambda_0=0.550 \text{ nm}$ ,  $\lambda_0=0.6328 \text{ nm}$  and  $\lambda_0=1.064 \text{ }\mu\text{m}$ . Figure 5 despite the transmission profile and Table (1) summarized the output data.

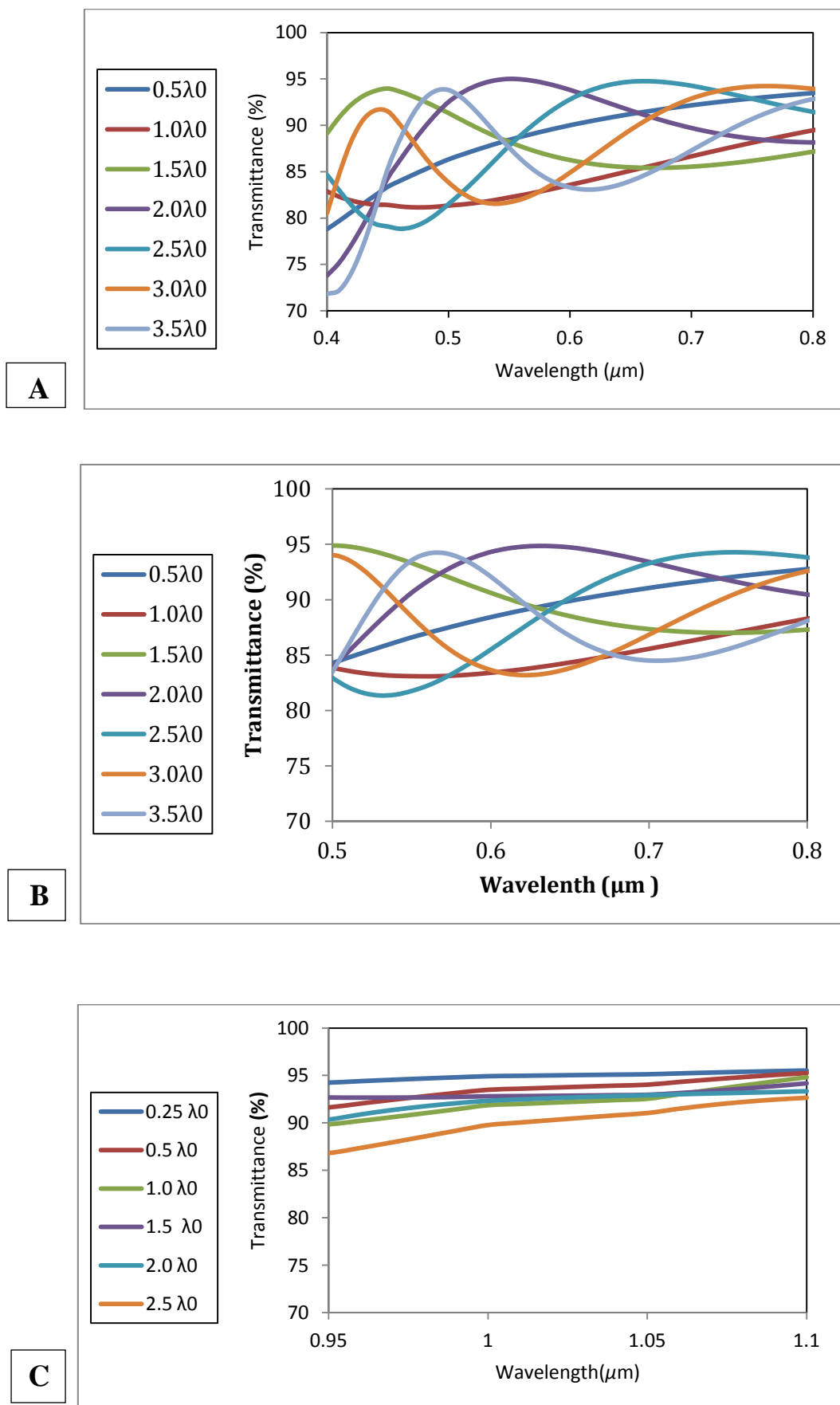


**Figure 5.** Computed transmittance of ITO /Glass at different design wavelength: (A)  $\lambda_0=0.550 \text{ nm}$ , (B)  $\lambda_0=0.6328 \text{ nm}$  and (C)  $\lambda_0=1.064 \mu\text{m}$ .

**Table 1** Output geometrical thickness and transmittance data

Optical thickness ( $\lambda_0$ )	$\lambda_0=0.55\mu\text{ m}$		$\lambda_0=0.6328\mu\text{ m}$		$\lambda_0=1.064\mu\text{ m}$	
	$d(\text{nm})$	T(%)	$d(\text{nm})$	T(%)	$d(\text{nm})$	T(%)
0.25	-	-	-	-	42.7	95.2
0.5	35.1	88.4	42.2	89.3	85.4	94.3
1.0	71.4	82.2	84.4	84.0	170.8	93.0
1.5	107.1	88.2	126.6	89.2	251.2	93.2
2.0	142.8	95.0	168.8	94.8	341.6	93.0
2.5	178.6	87.8	210.9	88.4	426.9	91.0
3.0	214.3	81.6	253.2	83.2	-	-
3.5	250.0	87.6	295.4	88.7	-	-

The tabulated results are gaining importance in providing us with a clear vision and preliminary geometrical thickness range of ITO material deposited on glass as substrate. In the process, we have eliminated the traditional standard practice in the conduct of research, which requires many attempts are subject to what is known as the (*Trial and error*) concept which causes wasted evident in the use of materials, techniques and devices testing and measurements.

### 3.3 Experimental Results

#### 3.3.1 Refractive Index And Extinction Coefficient

From experimental data of thin film preparation , the optical constants; refractive index  $n$  and extinction coefficient  $k$  of ITO film of different thickness range and impurity concentration ratios (5% and 10%) as a function of wavelength (0.400-1.10 $\mu\text{m}$ ) were investigated and shown in Figure 6.  $n$  and  $k$  curves show good stability in along wavelengths range (400-1100nm) which include three spectral regions, namely; ultraviolet, the visible region and near-infrared. Noting from Figure 6 that the refractive index and attenuation coefficient  $k$  for 5% concentration decreases as the wavelengths increased within the region under study. Furthermore the  $n$  values approaching glass refractive index for wavelengths greater than 700nm.

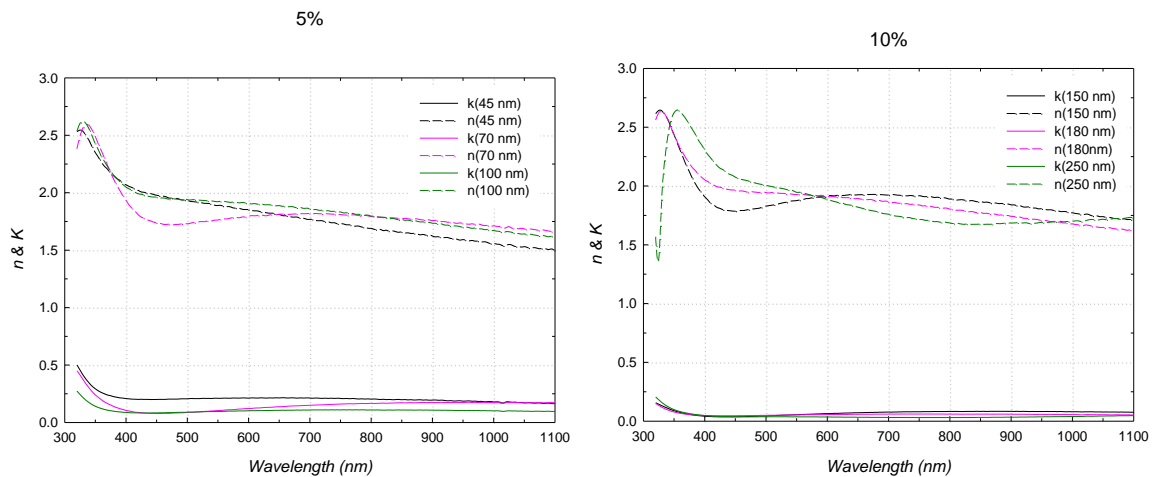


**Figure 6.** The effect of ITO thickness on the refractive index and extinction coefficient of film vs. wavelength for impurity ratios 5% and 10%.

The color map of the variation in  $n$  and  $k$  values results due to thickness and wavelength variation was shown in Figure 7.

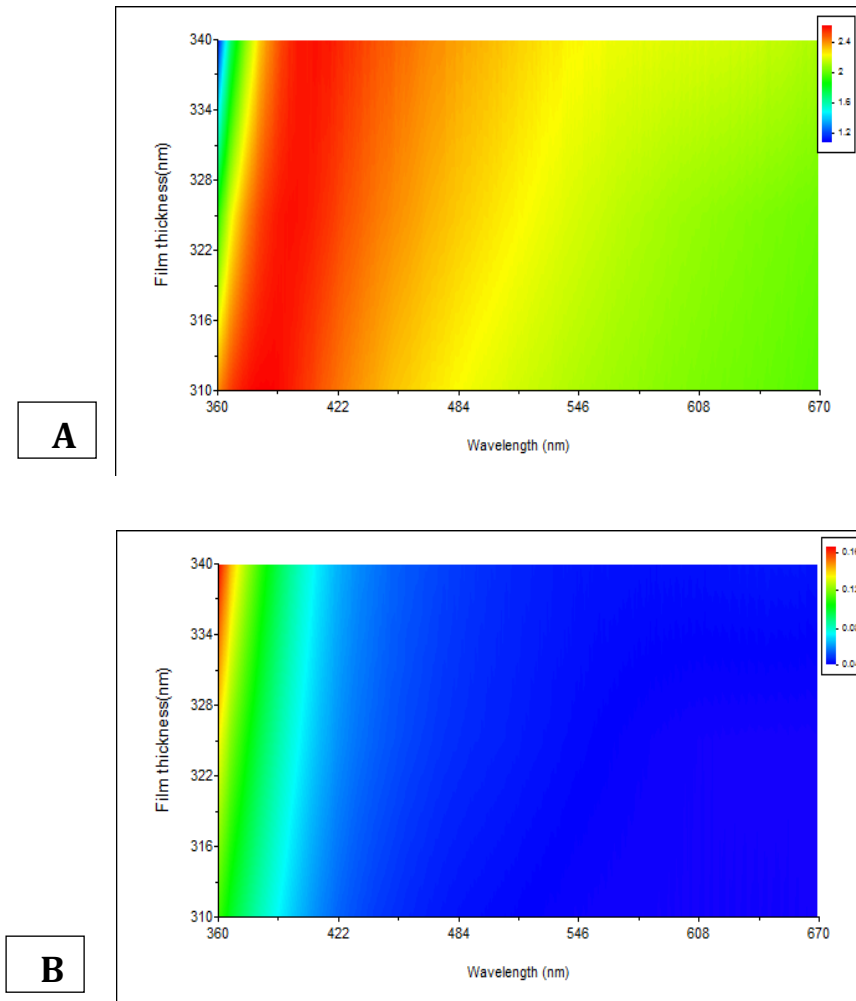


**Figure 7.** Contour lines of: (A)  $n$  - and (B)  $k$  - values due to thickness and wavelength variation.

### 3.3.2 Effect of Thickness Variation on Transmittance Profile

The behavior of decreasing refractive index  $n$  for wavelengths greater than 700nm is an important result, because it corresponds transmission increasing of ITO /glass at near-infrared wavelength as shown in Figure 8 and 9. For Nd-YAG laser line  $1.064\mu\text{m}$ . For 5% concentration the transmission of an assembly was 91.5% in comparison with that for uncoated glass which has 84.0%. The best measuring ITO thickness suitable for anti-reflective was ultra thickness of 45nm.



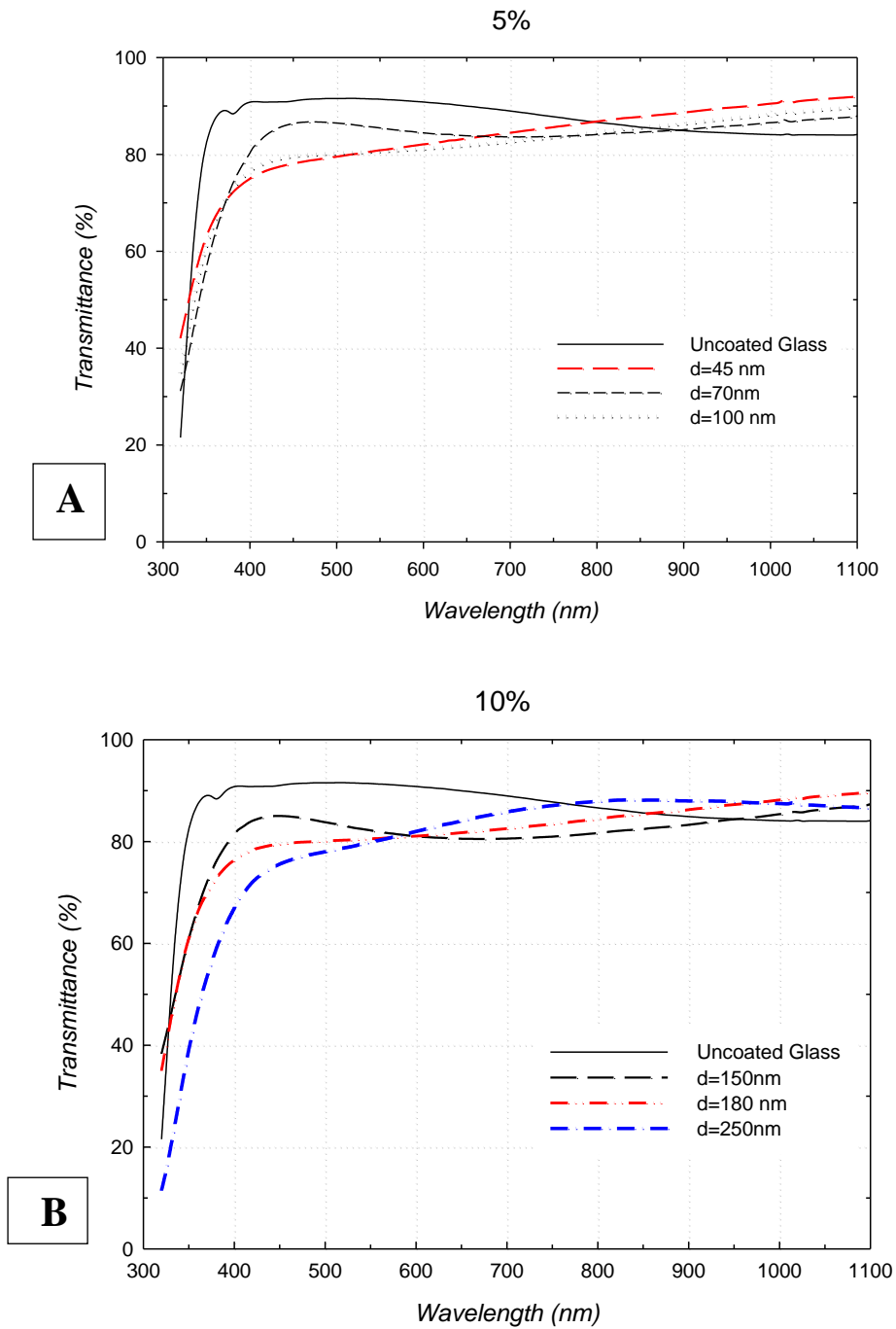


**Figure 8.** Effect of ITO thickness variation on the transmission of glass vs. wavelength for different concentration (A) 5%), (B) 10%.

*Transmission vs. Thickness*

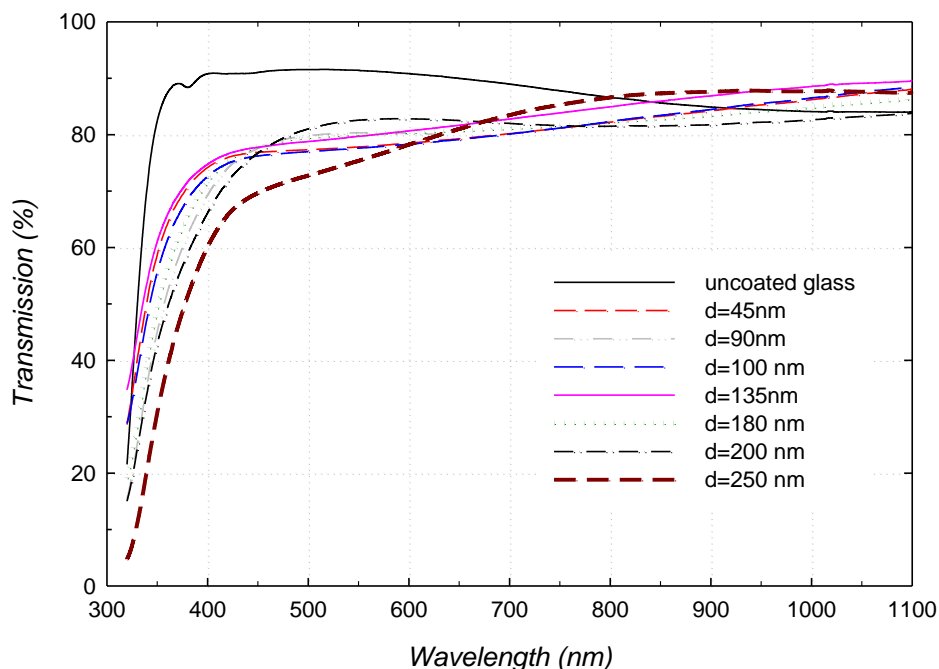


**Figure 9.** Measured transmission of ITO / glass vs. wavelength of 5% concentration over thickness range (45-250 nm).

#### 4. CONCLUSION

The current study has succeeded in overcoming two problems: the first, using high refractive , weakly absorbing ITO materials to obtain ultra-thin ARC's coating. This was achieved through the theoretical analysis of ITO/ glass transmission, which provides a clear vision and preliminary thickness range of ITO material before sample preparation. The second one the use of spray pyrolysis method for the first time to obtain ARC's of various optical constants through mixing materials with different concentrations.

#### ACKNOWLEDGMENTS

The authors would like to thank Mustansiriyah university for their support in this work

#### REFERENCES

- [1] Cul Yuanri, Xu Xinghao, Jin Zhaoting, Peng Chuancai and Xie Shuyun, Deposition of Transparent conducting Indium Tin Oxide Thin Films by Reactive Ion Plating, *Thin Solid Films* **115** (1984) 195-201.
- [2] C. H. L. Weujtens and P. A. C. Van Loon, Influence of Annealing on The Optical Properties of Indium Tin Oxide, *Thin Solid Films* **196** (1991) 1-10.
- [3] M. Losurdo, M. Giangregorio, P. Capezzuto, G. Bruno, R. De Rosa, F. Roca, C. Summonte, J. Plá & R. Rizzoli, Parametrization of optical properties of indium–tin–oxide thin films by spectroscopic ellipsometry: Substrate interfacial reactivity, *Journal of Vacuum Science & Technology A* **20** (2002) 37-42.

- [4] Yeon Sik Jung, Dong Wook Lee, Duk Young Jeon, Influence of dc magnetron sputtering parameters on surface morphology of indium tin oxide thin films, *Applied Surface Science* **221** (2004) 136–142.
- [5] A. Mohammadi Gheidari, E. Asl Soleimani, M. Mansorhoseini, S. Mohajerzadeh, N. Madani, W. Shams-Kolahi, Structural properties of indium tin oxide thin films prepared for application in solar cells, *Materials Research Bulletin* **40** (2005) 1303–1307.
- [6] C. Rhodes, M. Cerruti, A. Efremenko, M. Losego, D. E. Aspnes, J.-P. Maria & S. Franzen, Dependence of Plasmon Polariton of the Thickness of Indium Oxide thin Films, *Journal of Applied Physics* **103** (2008) 09310-6.
- [7] Lei Hao, Xungang Diao, Huaizhe Xu, Baoxia Gu, Tianmin Wang, Thickness dependence of structural, electrical and optical properties of indium tin oxide (ITO) films deposited on PET substrates, *Applied Surface Science* **254** (2008) 3504–3508.
- [8] Y. C. Lin, W. Q. Shi, Z. Z. Chen, Effect of deflection on the mechanical and optoelectronic properties of indium tin oxide films deposited on polyethylene terephthalate substrates by pulse magnetron sputtering, *Thin Solid Films* **517** (2009) 1701–1705.
- [9] Chih-Hao Lian, Sheng-Chau Chen, Xiaoding Qi, Chi-San Chen, Chih-Chao Yang, Influence of film thickness on the texture, morphology and electro-optical properties of indium tin oxide films, *Thin Solid Films* **519**(2010)345-350.
- [10] Federica Rigoni, Giovanni Drera, Stefania Pagliara, Andrea Goldoni, Luigi Sangaletti, High sensitivity, moisture selective, ammonia gas sensors based on single-walled carbon nanotubes functionalized with indium tin oxide nanoparticles, *Carbon* **80** (2014)356-363.
- [11] Maciej Mierzwa, Emmanuel Lamouroux, Ivan Vakulko, Pierrick Durand, Mathieu Etienne, Electrochemistry and Spectroelectrochemistry with Electrospun Indium Tin Oxide Nanofibers, *Electrochimica Acta* **202** (2016) 55-65.
- [12] F. O. Adurodija, H. Izumi, T. Ishihara, H. Yoshioka, M. Motoyama, K. Mura, Effect of laser irradiation on the properties of indium tin oxide films deposited by pulsed laser deposition, *Applied Surface Science* **177** (2001) 114-121.
- [13] Yan Song, Yuting Ma, Yuan Wang, Junwei Di, Yifeng Tu, Electrochemical deposition of gold-platinum alloy nanoparticles on an indium tin oxide electrode and their electrocatalytic applications, *Electrochimica Acta* **55** (2010) 4909–4914.
- [14] Adam W. Sood, David J. Poxson, Frank W. Mont, Sameer Chhajer, Jaehee Cho, E. Fred Schubert, Roger E. Welsler, Nibir K. Dhar, and Ashok K. Sood, Experimental and Theoretical Study of the Optical and Electrical Properties of Nanostructured Indium Tin Oxide Fabricated by Oblique-Angle Deposition, *Journal of Nanoscience and Nanotechnology* **12** (2012) 3950–3953.
- [15] W-F. Wu, B-S. Chiou, Mechanical and optical properties of ITO film with anti-reflective and anti-Wear coatings, *Applied Surface Science* **115** (1997) 96-102.
- [16] H. Kim, A. Pique, J. S. Horwitz, H. Mattoussi, H. Murata, Z. H. Kafafi, and D. B. Chrisey, Indium tin oxide thin films for organic light-emitting devices, *Applied Physics Letters* **74** (1999) 3444-3446.
- [17] Furong Zhu, Keran Zhang, Ewald Guenther, Chua Soo Jin, Optimized indium tin oxide contact for organic light emitting diode applications, *Thin Solid Films* **363** (2000) 314-317.
- [18] V. S. Vaishnav, P. D. Patel, N. G. Patel, Indium Tin Oxide thin film gas sensors for detection of ethanol vapours, *Thin Solid Films* **490** (2005) 94-100.
- [19] K. Vijayalakshmi, C. Ravidhas, V. Vasanthi Pillay, D. GopalaKrishna, Influence of deposition parameters and heat treatment on the NO<sub>2</sub> sensing properties of nanostructured indium tin oxide thin film, *Thin Solid Films* **519** (2011) 3378–3382.
- [20] Steven K. Hau, Hin-Lap Yip, Jingyu Zou, Alex K.-Y. Jen, Indium tin oxide-free semi-transparent inverted polymer solar cells using conducting polymer as both bottom and top electrodes, *Organic Electronics* **10** (2009) 1401–1407.

- [21] Chan-Shan Yang, Tsung-Ta Tang, Po-Han Chen, Ru-Pin Pan, Peichen Yu, and Ci-Ling Pan, Voltage-controlled liquid-crystal terahertz phase shifter with indium-tin-oxide nanowhiskers as transparent electrodes, *Optics Letters* **39** (2014) 2511-2513.
- [22] Di Guo, Ming Zhuo, Xiaoi Zhang, Cheng Xua, Jie Jianga, Fu Gaob, Qing Wana, Qihong Li, Taihong Wang, Indium-tin-oxide thin film transistor biosensors for label-free detection of avian influenza virus H5N1, *Analytica Chimica Acta* **773** (2013) 83-88.
- [23] He Tian, Dan Xie, Yi Yang, Tian-Ling Ren, Yu-Feng Wang, Chang-Jian Zhou, Ping-Gang Peng, Li-Gang Wang and Li-Tian Liu, Transparent, flexible, ultrathin sound source devices using Indium Tin oxide films, *Applied Physics Letters* **99** (2011) 043503-3.
- [24] Min Hyung Ahn, Eou-Sik Cho, Sang Jik Kwon, Effect of the duty ratio on the indium tin oxide (ITO) film deposited by in-line pulsed DC magnetron sputtering method for resistive touch panel, *Applied Surface Science* **258** (2011) 1242– 1248
- [25] Steven K. Hau, Hin-Lap Yip, Jingyu Zou, Alex K.-Y. Jen, Indium tin oxide-free semi-transparent inverted polymer solar cells using conducting polymer as both bottom and top electrodes, *Organic Electronics* **10** (2009) 1401–1407.
- [26] M. Balestrieri, D.Pysch, J.-P.Becker, M.Hermle, W.Warta, S.W.Glunz Characterization and optimization of indium tin oxide films for Heterojunction solar cells, *Solar Energy Materials & Solar Cells* **95** (2011) 2390–2399.
- [27] Anh Huy Tuan Le, Shihyun Ahn, Sangmyeong Han, Jungmo Kim, Shahzada Qamar Hussain, Hyeongsik Park, Cheolmin Park, Cam Phu Thi Nguyen, Vinh Ai Dao, Junsin Yi, Effective optimization of indium tin oxide films by a statistical approach for shallow emitter based crystalline silicon solar cell applications, *Solar Energy Materials Solar Cells* **125** (2014) 176–183.
- [28] Y. Gao, G. Zhao, Z. Duan, Y. Ren, Preparation of ITO films using a spray pyrolysis solution containing an acetylacetone chelating agent, *Materials Science-Poland* **32** (2014) 66-70.
- [29] H. A. Macleod, *Thin -film optical filters*, 4<sup>th</sup> ed. CRC Press (2010).
- [30] M.Born and E.Wolf, *Principle of optics*, 6<sup>th</sup> ed. Pergamon, London (1986).
- [31] A. Musset and A.Thelen, *Multilayer Antireflection Coatings*, in *progress in optics*, E.Wolf ed. North-Holland Amsterdam **18** (1970) 201-207.
- [32] W. G. Driscoll and W. Vaughan, *Handbook of optics* McGraw-Hill New York (2010).
- [33] R. J. Moerland and Jacob P. Hoogenboom, Sub-nanometer-accuracy optical distance ruler based on fluorescence quenching by transparent conductors, *Optica* **3** (2016) 112-117.
- [34] [www.refractiveindex.info](http://www.refractiveindex.info)
- [35] Y.S. Jung, Spectroscopic ellipsometry studies on the optical constants of indium tin oxide films deposited under various sputtering conditions, *Thin Solid Films* **467** (2004) 36–42.
- [36] <https://spectra.com>